# Lamellar Mesogels and Mesophases: A Self-Consistent-Field Theory

**E. B. Zhulina† and A. Halperin*,‡**

*Institut für Physik, Johannes Gutenberg University Mainz, Staudinger Weg 7, W-6500 Mainz, Germany, and Materials Department, University of California at Santa Barbara, Santa Barbara, California 93106*

*Received March 13, 1992*

ABSTRACT: A fundamental distinction between the mesophases formed by ABA triblock copolymers and by AB diblock copolymers is the occurrence of B bridges between A domains. The ABA mesophases form physically cross-linked networks characterized by a nonuniform spatial distribution of high-functionality cross-links. The swelling of these networks by selective solvents gives rise to novel "mesogels". Two theoretical aspects of these systems, focusing on the lamellar case, are considered: (i) the equilibrium fraction of bridging chains in mesophases formed by a melt of ABA triblock copolymers; (ii) the swelling equilibrium and the deformation behavior of mesogels swollen by a selective solvent for the B blocks as a function of the fraction of bridging B chains.

## I. Introduction

The mesophases formed by diblock and triblock copolymers are, in certain respects, indistinguishable. Thus, the microphase separation of $A_MB_{2N}A_M$ triblock and $A_MB_N$ diblock copolymers results in domains of identical size and symmetry.[1] Yet, the two systems are fundamentally different because the mesophases formed by triblock copolymers involve bridging of A domains by B blocks. This qualitative distinction is of practical interest because ABA triblocks form industrially important thermotropic elastomers.[2] The effect of the bridging is also manifested in the behavior of these systems in the presence of a selective solvent for the B blocks: Mesophases of AB diblock copolymers dissolve while those formed by ABA triblock copolymers are expected to swell, thus forming physical gels.[3-5] Such physical gels are expected to be long lived when the insoluble A domains are glassy or crystalline in the experimental regime. Since these novel gels retain some of the characteristic features of the original mesophases, we refer to them as *mesogels*. In particular, the cross-links involve the insoluble A domains and the mesogels are thus characterized by cross-links of high functionality and anisotropic distribution in space. For example, the cross-links of a lamellar gel are constrained to planes while those of a cylindrical gel are constrained to lines. The elementary subunits of mesogels are thus highly branched assemblies of flat, cylindrical, or spherical geometry. These subunits comprise, in essence, densely grafted layers;[6] i.e., since the A-B junctions are constrained to the interface of the A domains, the soluble B blocks are terminally anchored to a sphere, a cylinder, or a flat layer consisting of insoluble A blocks. In marked distinction typical model gels are characterized by a uniform distribution of cross-links of low functionality.[7,8] The following theoretical discussion is confined to lamellar mesogels and mesophases formed by ABA triblock copolymers. We first consider the *fraction of bridging B chains in equilibrium* $q_{eq}$. However, experimentally the system may fail to attain $q_{eq}$ because of the kinetics of segregation. Thus, our subsequent discussion of the resulting mesogels allows for an arbitrary fraction of bridging B blocks, $q$. This discussion concerns the *swelling equilibrium and the deformation behavior of the lamellar gels* with special emphasis on the *q dependence of the elastic moduli*. This last problem is amenable to self-consistent-field treatment but is difficult to analyze within the framework of simpler models. The analysis is focused on the behavior of "single crystal" samples comprised of flat, well-aligned lamellae. Such samples are obtainable by application of shear fields to the melt mesophase.[5] After the preparation stage the sample is cooled down to a temperature in which the A domains are glassy while the B domains remain rubbery. It is assumed that the structure obtained corresponds to the strong segregation limit; i.e., the thickness of the AB interface is comparable to monomer size, and the associated surface tension, $\gamma$, is independent of $N$ and $M$. The mesogels considered are obtained by swelling the resulting single-crystal lamellar phase by a highly selective solvent: a good solvent for the B blocks and a precipitant for the A blocks. It is assumed that the swelling does not modify the structure of the insoluble and glassy A domains. In particular, $\sigma$, the area per A-B junction at the AB interface, and $q$ are assumed to retain their initial values. For simplicity it is also assumed that the flexible and neutral triblock copolymers are perfectly monodispersed comprising A blocks consisting of $M$ monomers and B blocks incorporating $2N$ monomers. The foundation of the discussion is the view of the B layer as a brush of densely grafted chains. This justifies the use of the self-consistent-field theory of dense brushes as pioneered by Semenov.[9]

The problem outlined above is of interest from a number of viewpoints. As noted earlier, it concerns both fundamental and practical aspects of the phase behavior of block copolymers. These aspects involve the formation of a physical network due to B blocks bridging different A domains. The behavior of swollen mesogels provides an additional probe of the bridging chains. The system considered is also of interest because it provides a macroscopic realization of densely grafted brushes. In turn, polymer brushes attract considerable current interest because of the stretched configurations adopted by densely grafted chains and their manifestations in phase behavior, dynamics, etc.[6] The deformation behavior of polymer brushes is currently studied by means of a force measurement apparatus. However, the study of sheared and stretched brushes is hampered by complications due to dynamical effects. The use of lamellar mesogels as model systems should enable the study of stretched or sheared brushes under static conditions. Another perspective is that of physical gelation. This often involves a block structure in the participating chains (for example, helical and coillike blocks).[10] This suggests the study of gel

† Johannes Gutenberg University Mainz.
‡ University of California at Santa Barbara.

0024-9297/92/2225-5730$03.00/0 

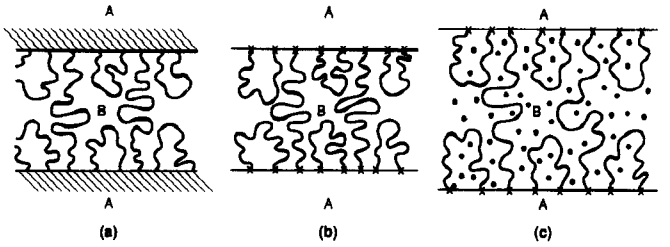


**Figure 1.** Route to lamellar mesogels: (a) Preparation of an aligned sample of a lamellar phase in a melt state. (b) "Fixation" of the A domains by quench below $T_g$ of the A polymers, selective cross-linking, etc. (c) Swelling by a selective solvent for the B blocks.

formation by multiblock copolymers in a selective solvent as a model system.[11] However, the first and simplest step in this direction is clearly the study of physical gelation by ABA triblock copolymers. The final source of interest is the study of polymer networks. Aligned lamellar mesogels exhibit a number of interesting traits traceable to the distinctive characteristics of the cross-links.[3,4] Among them are an anisotropic deformation behavior, asymmetry of compression and extension, and nonaffine deformation behavior in good solvents. The extension of lamellar mesogels in poor solvent is expected to exhibit a regime where the stress is independent of the strain. This plateau in the stress–strain diagram is due to the associated first-order phase transition.[4,12,13]

The paper is organized as follows. The equilibrium structure of lamellar mesophases formed by a melt of ABA triblock copolymers is considered in section II. This section also introduces Semenov's SCF formalism while delegating the formal details to Appendix I. The next section reviews the behavior of lamellar gels as revealed by scaling arguments. The discussion follows, with certain refinements, the presentation of refs 3, 13, and 14. The SCF theory of swollen lamellar mesogels is described in section IV while the mathematical details are summarized in Appendix II. The swelling equilibrium and the deformation behavior of lamellar gels are analyzed in section V by means of force balance arguments. A summary of the experimental situation and suggestions for future experiments are presented in the Discussion.

## II. Copolymeric Mesophases: Triblocks vs Diblocks

Mesophases formed by ABA triblock copolymers exhibit bridging of A domains by B blocks (Figure 1). This is an important feature since it results in the formation of physically cross-linked networks. The phenomen is also of fundamental interest as a qualitative difference between the mesophases formed by diblock and triblock copolymers. These mesophases are otherwise quite similar with regard both to symmetry and to the characteristic dimensions of the domains. A theoretical model for this phenomenon must account for the various options available to the B blocks. If each of the A blocks belongs to a different domain, the B block forms a bridge. When the two A blocks are incorporated into a single domain, the B block forms a loop. In this case one must allow for the possibility of bridging due to entanglements between loops anchored to different domains. Finally, one of the A blocks may be embedded in a B domain, giving rise to a "dangling end". This last option may be neglected in the strong segregation limit considered here. In the following we aim to obtain the equilibrium ratio of bridges and loops in a strongly segregated lamellar phase. As we shall see the theory does not distinguish between entangled loops and direct bridges for the case of a perfectly monodispersed sample.

It is convenient to begin with a brief review of the structure of lamellae formed by diblock copolymers, in particular, flexible, symmetric AB diblock copolymers incorporating $2N$ monomers. The lamellar structure reflects the interplay between the intrafacial energy associated with the AB boundary, $F_{sur}$, and the deformation penalties, $F_A$ and $F_B$, due to the stretching of the grafted A and B blocks.[6,14] The excess free energy per copolymer is

$$F = F_A + F_{sur} + F_B \qquad \text{(II.1)}$$

where the reference state is of the disconnected blocks in a melt of identical chains. The intrafacial term is simply given by $\sigma\gamma$ where $\sigma$ is the surface area per block. The Alexander model[15] yields a simple approximation for the deformation penalties. All chains are assumed to be uniformly stretched. The end to end distance of each block is thus equal to the thickness of the layer, $H$. In turn, $H$ is related to $\sigma$ by the incompressibility condition $H\sigma = Na^3$. The deformation term is then given by the elastic free energy of a Gaussian coil, $kTH^2/Na^2 \approx kTNa^2/\sigma^2$. Minimization with respect to $\sigma$ yields the equilibrium characteristics of the layer

$$H/a \approx (\gamma a^2/kT)^{1/3}N^{2/3} \qquad \text{(II.2)}$$

and

$$\sigma/a^2 \approx (kT/\gamma a^2)^{1/3}N^{1/3} \qquad \text{(II.3)}$$

While this model accounts rather successfully for the experimental results, it is clearly too restrictive. The uniform stretching assumption places an undue constraint on the chains, and the resulting free energy is thus overestimated. A more realistic approach, allowing the chain ends to be anywhere within the layer, was recently devised by Semenov.[9,16] This self-consistent-field (SCF) analysis recovers the results obtained by the Alexander approach apart from slightly different multiplicative constants. While the SCF approach did not yield qualitatively new results for aggregates of diblock copolymers, it is, as we shall see, crucial for a proper analysis of mesophases formed by triblock copolymers. The Alexander model can account for certain properties of triblock copolymer mesophases. For example, it accounts successfully for the characteristic dimensions of the domains. Its implementation for lamellae formed by symmetrical $A_MB_{2N}A_M$ triblock copolymers is particulary simple. The lamella is considered to be equivalent to two lamellae formed by $A_MB_N$ diblock copolymers. However, the Alexander approach fails to predict the correct ratio of bridging and nonbridging B blocks. The SCF anaysis suggests a different picture for the B layer. Within this picture the layer consists of three regions: (i) a central region where only bridging chains are present (in this region the chains are uniformly stretched); (ii) two boundary layers which contain both bridging and nonbridging chains (in these layers the stretching is nonuniform). In contrast to the Alexander model the free energy of the bridging chains is higher than that of nonbridging chains and their fraction is correspondingly lower. This picture was first presented by Johner and Joanny[17] for a swollen brush with adsorbing end groups in the presence of a surface. A similar analysis was presented by Ligoure et al.[18] for a solution of telechelic polymers between two walls. Our analysis follows the discussion of Zhulina and Pakula[19] of a melt of grafted chains with adsorbing end groups interacting with a surface.

To present the SCF analysis consider a B layer comprised of blocks consisting of $2N$ monomers such that the area

per anchored end group is $\sigma$. Since the layer is symmetric with respect to the midplane, it is sufficient to consider half of the layer, of thickness $H_0 = Na^3/\sigma$. The thickness of the boundary layer is denoted by $h$ and the fraction of bridging chains by $q$. Each bridging chain deposits $N'$ monomers within the boundary layer. The remaining chains are nonbridging loops. In the following a loop is treated as two linear chains each comprised of $N$ monomers. We aim to characterize the equilibrium structure of the B layer for given values of $q$ and $N'$. These determine $h$ since a volume of $(H_0 - h)\sigma$ in the central region contains $q(N - N')$ monomers of volume $a^3$, thus leading to

$$h/H_0 = 1 - q\tau \tag{II.4}$$

where $\tau = (N - N')/N$ is the fraction of monomers, belonging to a bridging chain, which are deposited in the central layer. The bridging chains in the central region are uniformly stretched. The elastic free energy per copolymer due to the chain segments embedded in the central layer is thus

$$F_c/kT = 3q(H_0 - h)^2/2(N - N')a^2 \tag{II.5}$$

The corresponding tension is

$$f_c/kT = 3(H_0 - h)/(N - N')a^2 \tag{II.6}$$

The chains in the boundary layer are not uniformly stretched, and its description is accordingly more complex. The average elastic free energy per chain in the boundary layer is

$$F_b/kT = (1 - q)(3/2a^2)\int_0^h d\eta\, g(\eta) \int_0^\eta E_n(x,\eta)\, dx + q(3/2a^2)\int_0^h E_b(x,h)\, dx \tag{II.7}$$

$E_n(x,\eta) = dx/dn$ is, essentially, the local tension in a chain whose end point is located at height $\eta$. The tension is actually given by $f_b = kT(3/a^2)E$. The representation of the local elastic free enrgy as $E(\mathbf{r},\mathbf{r}')\, d\mathbf{r}$[9] is identical to the familar $E^2(\mathbf{r},\mathbf{r}')\, dn$.[20] However, in our case $E(\mathbf{r},\mathbf{r}')\, d\mathbf{r}$ is replaced by a one-dimensional form $E(x,\eta)\, dx$ because of the stretched configurations adopted by the grafted B blocks. These are also reflected in the requirement that $x < \eta$. These simplications are possible because the stretching reduces the number of configurations accessible to the coil. The possible configurations may be considered as weak fluctuations around a single dominant trajectory. Thus, if the accessible configurations of a weakly deformed chain are reminiscent of the possible trajectories of a quantal particle, the configurations of a stretched chain are analogous to the trajectory of a classical particle. $E_b(x,h) = E_b(x)$ is the local tension in bridging chains whose end points are always positioned at the periphery of the boundary layer. $E_n(x,\eta)$ is the local tension in a nonbridging chain whose end is located at height $\eta \le h$. The end points of such chains are distributed throughout the boundary layer, and $g(\eta)$ is the corresponding height distribution function.

In order to find the equilibrium state of the boundary layer, it is necessary to minimize the free energy given by (II.7) subject to the following constraints:

$$\int_0^\eta E_n^{-1}(x,\eta)\, dx = N \tag{II.8}$$

$$\int_0^h E_b^{-1}(x)\, dx = N' \tag{II.9}$$

and

$$\Phi(x) = (1 - q)(a^3/\sigma)\int_x^h g(\eta)\, E_n^{-1}(x,\eta)\, d\eta + qa^2/\sigma E_b(x) = 1 \tag{II.10}$$

Constraints (II.8) and (II.9) assure the conservation of monomers for bridging and nonbridging chains. The constant melt density within the layer is reflected in (II.10). Note the choice of the integration domain in the first term of (II.10) stating that monomers at height $x$ may only originate in nonbridging chains with end points at a greater height $\eta$, $x < \eta < h$. This is another manifestation of the stretched configurations of the grafted B coils. The constraints are supplemented by the requirements of mechanical equilibrium which impose equality of the tension at the edge of the boundary layer to the tension in the central region.

$$E_b(h) = (H_0 - h)/(N - N') \tag{II.11}$$

The details of the calculation are described in Appendix I. The equilibrium structure of the boundary layer, for a given set of $\sigma$, $N'$, and $q$, is specified by

$$E_n(x,\eta) = (\pi/2N)(\eta^2 - x^2)^{1/2} \tag{II.12}$$

$$E_b(x,h) = (\pi/2N)(\Lambda^2 - x^2)^{1/2} \tag{II.13}$$

where $\Lambda = h/\cos(\pi\tau/2)$. The distribution function for the free chain ends is

$$g(\eta) = \frac{1}{(1 - q)H_0}\frac{\eta(h^2 - \eta^2)^{1/2}}{\Lambda^2 - \eta^2} \tag{II.14}$$

For $q = \tau = 0$ (II.14) reduces to the $g(\eta)$ of a dense brush of free chains. The combination of (II.4), (II.11), and (II.13) specifies the interdependence of $q$ and $\tau$

$$2q/\pi \tan(\pi\tau/2) = 1 - q\tau \tag{II.15}$$

Knowing $E_n(x,\eta)$, $E_b(x)$, and $g(\eta)$, it is possible to obtain the elastic energy per chain, $F_{el} = F_b + F_c$.

$$F_{el}/kT = (F_{el}^0/kT)[(1 - \tau q)^3 + (12/\pi^2)q^2] \tag{II.16}$$

where $F_{el}^0/kT = (\pi^2/8)(Na^4/\sigma^2)$ is the elastic free energy of a free ($q = 0$) dense brush.[4] Taking (II.15) into account, one obtains $F_{el}$ for small $q$ values, $q \ll 1$.

$$F_{el}/kT = (F_{el}^0/kT)[1 + (2q/\pi)^4] \tag{II.17}$$

Apart from the elastic free energy, it is necessary to account for the mixing entropy of bridging and nonbridging chains. The free energy per chain, $F_{chain}$, assuming random mixing is

$$F_{chain}/kT = F_{el}/kT + q \ln q + (1 - q) \ln (1 - q) \tag{II.18}$$

Note that the mixing entropy term is actually an upper bound. It assumes that the head groups of the loops are uncorrelated. In reality the two head groups of each loop are connected by a flexible coil. A lower bound for the mixing entropy is obtained by considering such pairs as rigid dimers. The corresponding mixing term is $q \ln q + (1/2)(1 - q) \ln (1 - q)$. However, this refinement is not important for the scaling behavior of $q_{eq}$. Minimization of (II.18) with respect to $q$, assuming that $q$ is small, leads to $q \approx 1 - q^3(F_{el}/kT)$. Accordingly $q^3(F_{el}^0/kT)$ is of order unity and the equilibrium value of $q$, $q_{eq}$, for a given $\sigma$[4] is

$$q_{eq} \approx (kT/F_{el}^0)^{1/3} \approx (\sigma/a^2)^{2/3}N^{-1/3} \tag{II.19}$$

It is however important to note that the kinetics of phase separation may prevent $q$ from reaching its equilibrium value. This is particularly true for samples aligned by

shear fields. The application of shear may actually enhance bridging, as is the case for associating polymers and micelles.[21,22]

## III. Mesogels: A Scaling Description

Mesogels are obtainable from any of the mesophases formed by ABA triblock copolymers. It is thus possible to envision lamellar, cylindrical, and micellar gels.[3,4] Their detailed structure depends on the nature of the A blocks. These may be flexible, rigid, or crystallizable. The characteristic dimensions of the A domains are somewhat different for each case. We mostly consider lamellar gels formed from crystalline–coil–crystalline ABA triblock copolymers. The special features of lamellar gels are most evident in "single-crystal" samples, i.e., aligned mesogels where the A domains are parallel. The discussion is limited to such samples. It is concerned, primarily, with their macroscopic characteristics: swelling equilibrium and deformation behavior as revealed by the scaling approach.[3,4,12,13] We summarize the behavior in good, Θ, and poor solvents. For simplicity the A domains are assumed to be perfectly rigid. In particular, they are assumed to retain their equilibrium dimensions as attained in the melt mesophase. The preceding section outlined the factors determining the equilibrium fraction of bridging B blocks, $q_{eq}$. The actual fraction, $q$, may be quite different since it probably depends on the history of the sample. For simplicity we mostly focus on the idealized limit of $q = 1$ obtained when all B blocks bridge different A domains. For the same reason we ignore, at this early stage, complications due to entanglements, defects, nonuniformities, etc.

Single-crystal lamellar gels swell uniaxially, along the lamellar normal. Since the B blocks are densely grafted to the interface of the A domains, the B layer is structurally similar to a brush. The equilibrium swelling of the gel corresponds to a fully swollen brush. In a good solvent the swollen brush is envisioned as an array of close-packed concentration blobs of cross section $\sigma$. Each chain, when viewed as a string of blobs, is strongly stretched. It is, in effect, confined to a cylindrical capillary of cross section $\sigma$. The thickness of the brush is thus $H_{eq} \approx (N/g)\sigma^{1/2}$ where $g$ is the number of monomers per blob. In a good solvent the blob size is given by $\xi \approx v^{1/5}g^{3/5}a \approx v^{-1/4}\Phi^{-3/4}a$ where $va^3$ is the second virial coefficient and $H_{eq}$ is thus

$$H_{eq} \approx v^{1/3}N(a^2/\sigma)^{1/3}a \qquad \text{(III.1)}$$

while the monomer volume fraction in the layer $\Phi_{eq} \approx Na^3/\sigma H_{eq}$ is

$$\Phi_{eq} \approx v^{-1/3}(a^2/\sigma)^{2/3} \qquad \text{(III.2)}$$

For crystalline A domains, when $\sigma \sim N^{1/3}$,[23] we thus have[3] $\Phi_{eq} \sim N^{-2/9}$ as compared to $\Phi_{eq} \sim N^{-4/5}$ for simple gels.[7,8] The free energy per chain, in this regime, is comprised of two terms: an interaction free energy, $(N/g)kT$, obtained by assigning $kT$ to each blob, and an elastic penalty due to the deformation of a Gaussian string of blobs from $R_0 \approx (N/g)^{1/2}\xi$ to $H$.

$$F_{chain}/kT \approx v^{-1/4}(H^2/Na^2)\Phi^{1/4} + v^{3/4}N\Phi^{5/4} \approx v^{3/4}\Phi_{eq}{}^{9/4}(\sigma/a^2)(H_{eq}/a)[(H/H_{eq})^{7/4} + (H_{eq}/H)^{5/4}] \qquad \text{(III.3)}$$

The compression of the layer gives rise to a restoring force per chain, $f = -\partial F_{chain}/\partial H$. The pressure, $G_N = f/\sigma$, is thus

$$G_N a^3/kT \approx v^{3/4}\Phi_{eq}{}^{9/4}[(H_{eq}/H)^{9/4} - (H/H_{eq})^{3/4}] \qquad \text{(III.4)}$$

In this regime the B layer is viewed as a slab of semidilute solution. It is however different from a semidilute solution of free polymers because the chains are stretched. The restoring pressure for strong compression is dominated by the osmotic term, $G_N \sim (H_{eq}/H)^{9/4}$. This result is independent of $q$. The same law obtains for $q = 1$ and for the compression of two disconnected brushes, $q = 0$. The stretching behavior is markedly different. Since the chains in equilibrium state are envisioned as fully stretched strings of blobs, further extension is only possible upon rearrangement of the blob structure. A description of this regime was suggested recently by Rabin and Alexander,[24] who generalized an earlier approach due to Pincus.[8,25] Each chain is pictured as a fully stretched string of Pincus blobs of size $\xi_p$ determined by $\xi_p f \approx kT$ where $f$ is the tension in the chain. For sufficiently weak deformations the blobs exhibit self-avoidance and each blob incorporates $g_p \approx v^{-1/5}(\xi_p/a)^{5/3}$ monomers. Accordingly, the chain length is $H \approx (N/g_p)\xi_p \approx v^{1/3}N(fa/kT)^{2/3}a$ and its elastic free energy, as given by the $kT$ per blob prescription, is $(N/g_p)kT \approx v^{1/3}N(fa/kT)^{5/3}kT$. However, $\xi_p < \sigma^{1/2}$, while the volume per chain, $\sigma H$, is larger then $\sigma H_{eq}$. Accordingly, the blobs are not close-packed, and the familiar $kT/\xi^3$ ansatz for the interaction free-energy density fails. An alternative approach utilizes a Flory type argument allowing for blob–blob interactions: Each blob experiences an interaction energy of $kT\Phi_p$ where $\Phi_p \approx \xi_p{}^2/\sigma$ is the blob volume fraction. The interaction energy in a good solvent is repulsive. The interaction free energy per chain is thus $N(a^2/\sigma)(a/\xi_p)^{1/3}kT$, and the total free energy per stretched chain is

$$F_{chain}/kT \approx v^{3/4}\Phi_{eq}{}^{9/4}(\sigma/a^2)(H_{eq}/a)[(H/H_{eq})^{5/2} + (H_{eq}/H)^{1/2}] \qquad \text{(III.5)}$$

The corresponding restoring pressure is

$$G_N a^3/kT \approx v^{3/4}\Phi_{eq}{}^{9/4}[(H/H_{eq})^{3/2} - (H_{eq}/H)^{3/2}] \qquad \text{(III.6)}$$

This regime occurs in a limited domain. For strong extensions the blobs are too small to experience excluded-volume interactions. As a result a new regime, characterized by Gaussian Pincus blobs, appears.[4] The boundary is specified by $\xi_p \approx r_b$ where $r_b \approx a/v$ is the size of a Gaussian blob comprised of $g_b$ monomers such that the monomer–monomer interactions are of order $kT$; i.e., $vg_b{}^2/r_b{}^3 \approx vg_b{}^{1/2} \approx 1$. The free energy per chain in the very strong stretching regime is

$$F_{chain}/kT \approx R_0{}^2/\sigma + (H/R_0)^2 \approx (H/R_0)^2 \qquad \text{(III.7)}$$

where the first term accounts for the interaction free energy $(N/g_p)(\xi_p{}^2/\sigma)kT$ and the second for the deformation penalty of a Gaussian coil.

The behavior of a brush in a Θ solvent is somewhat different. In this regime,[30] of $|v| < (a^2/\sigma)^{1/2}$, the interaction free energy is dominated by ternary encounters and the free energy per chain is

$$F_{chain}/kT \approx H^2/Na^2 + wN\Phi^2 = \Phi_\Theta{}^3(H_\Theta/a)[(H/H_\Theta)^2 + (H_\Theta/H)^2] \qquad \text{(III.8)}$$

where $w \approx 1$ is the third virial coefficient. The first term accounts for the stretching of a Gaussian chain and the second for ternary interactions between the monomers. The equilibrium characteristics of a brush in a Θ solvent are

$$H_\Theta \approx N(a^2/\sigma)^{1/2}a \qquad \text{(III.9)}$$

$$\Phi_\Theta \approx (a^2/\sigma)^{1/2} \qquad \text{(III.10)}$$

The corresponding restoring pressure is

$$G_N a^3/kT \approx \Phi_\theta^3[(H/H_\theta) - (H_\theta/H)^3] \quad \text{(III.11)}$$

The deformation behavior of a collapsed brush immersed in a poor solvent is richer. In particular, one expects a first-order phase transition, giving rise to a plateau in the stress–strain diagram. An indication for the occurrence of a phase transition is to be found in the Alexander model for a uniform brush in a poor solvent.[4] The free energy per chain, using the Flory exponents, is

$$F_{chain}/kT \approx H^2/Na^2 + N(-|v|\Phi + \Phi^2) \quad \text{(III.12)}$$

where $\Phi = Na^3/\sigma H$ is the monomer volume fraction. The first term accounts for the Gaussian elasticity of the chains, and the second reflects binary as well as ternary interactions between the monomers. Since we aim to characterize the $fH$ diagram, it is helpful to express $F_{chain}$ in terms of the tension $f/kT \approx H/Na^2 \equiv a^{-2}E$. This leads to

$$F_{chain}/NkT \approx E^2 - |v|a^3/\sigma E + a^6/\sigma^2 E^2 \quad \text{(III.13)}$$

The condition $\partial F_{chain}^2/\partial^2 E = \partial F_{chain}^3/\partial E^3 = 0$ reveals a critical point at

$$|v_c| \approx a/\sigma^{1/2}; \quad E_c \approx a(a^2/\sigma)^{1/2} \quad \text{(III.14)}$$

suggesting that a first-order phase transition occurs for $v < -|v_c|$.

A more detailed description of the "stretching transition" is desirable. This requires a clear picture of the collpased brush. A convenient description is possible in terms of blobs. In a poor solvent the discussion is based on collapsed blobs of size $\xi_c \approx g_c^{1/2}a$.[26,27] Each blob incorporates $g_c$ monomers exhibiting Gaussian statistics. $g_c$ is determined by the requirement that the attractive interactions within the blobs are comparable to $kT$; i.e., $(va^3/kT)(g_c^2/\xi_c^3) \approx g_c^{1/2}|\Delta T|/T_\theta \approx 1$ where $va^3/kT \approx v_0(\Delta T/T_\theta)$ is the second viral coefficient, $T_\theta$ is the $\Theta$ temperature, and $\Delta T = T - T_\theta$. Limiting ourselves to the case of $\sigma > \xi_c^2$, we may picture the layer as a close-packed array of $\xi_c$ blobs. The layer thickness, $H_c$, is given by[13,28-30]

$$H_c \approx N(a^2/\sigma)\xi_c \quad \text{(III.15)}$$

As in the good solvent case the chains are, in effect, confined to capillaries of cross section $\sigma$. However, in a brush swollen by a good solvent the blob size is $\xi \approx \sigma^{1/2}$ while in the poor solvent case $\xi_c$ is independent of $\sigma$. The expression for the thickness of the layer corresponds thus to a string of $N/g_c$ close-packed $\xi_c$ blobs within a cylinder of diameter $\sigma^{1/2}$. The density within the collapsed brush, $g_c a^3/\xi_c^3$, is equal to that of the dense phase resulting from polymer precipitation. The interface of the layer is associated with a surface tension of $\gamma \approx kT/\xi_c^2$.

The deformation behavior of the collapsed brush involves three stages:[3,4,13] (i) For small extensions, $H = H_c + \delta H \approx H_c$, a linear response is expected. The initially flat brush boundary develops "goose pimples", hemispherical deformations of height $\delta H$ and basal area $\sigma/q$. The linear restoring force, $f \sim \delta H$, is due to the associated increase in surface energy. (ii) The following stage is a first-order phase transition. It involves a coexistence of a dense, weakly deformed layer and a dilute layer of strongly stretched chains. The coexistence curve is obtained by equating the chemical potential of monomers in the two phases for a given $H$. The free energy per chain due to the $N_d$ monomers embedded in the dense layer is

$$F_d/kT \approx -N_d/g_c + (\sigma/q + \delta H^2)/\xi_c^2 \quad \text{(III.16)}$$

The term assigns an attractive energy of $-kT$ to each $\xi_c$ blob. For $N_d = N$, $F_d$ is the free energy of the weakly deformed layer described in (i). The corresponding chemical potential, $\mu_d = \partial F_d/\partial N_d$, is

$$\mu_d/kT \approx -g_c^{-1} \quad \text{(III.17)}$$

The remaining $N_s = n - N_d$ monomers form a stretched string of Pincus blobs of size $\xi_s$. In a poor solvent the blobs are Gaussian; i.e., $\xi_s \approx g_s^{1/2}a$ where $g_s$ is the number of monomers in a blob. When the lateral fluctuations of these strings, $\langle \Delta r^2 \rangle \approx Na^2$, are larger than $\sigma/q$, chain–chain interactions occur. The free energy per chain due to the stretched segment is

$$F_s/kT \approx H_s^2/N_s a^2 - (N_s/g_s)q\xi_s^2/\sigma \quad \text{(III.18)}$$

The first term, $H_s^2/N_s a^2 \approx N_s/g_s$, where $H_s \approx (N_s/g_s)\xi_s$ is the thickness of the dilute layer, accounts for the elastic free energy by assigning $kT$ to each Pincus blob. Chain–chain interactions give rise to the second term. Following Rabin and Alexander, each blob is assumed to experience interaction energy of order $kT\Phi_b$ where $\Phi_b \approx q_s^2/\sigma$ is the volume fraction of blobs. However, in the poor solvent case the blob–blob interaction is attractive rather than repulsive. The chemical potential, $\mu_s = (\partial F_s/\partial N_s)_H$, is

$$\mu_s/kT = -g_s^{-1} - qa^2/\sigma \quad \text{(III.19)}$$

The equality of the chemical potentials, $\mu_s = \mu_d = \mu$, leads to $g_s^{-1} = g_c^{-1} = qa^2/\sigma$ and to $\xi_s = \xi_c(1 - q\xi_c^2/\sigma)^{-1/2}$. This specifies $F_d$ and the tension, $f$, in the stretched chains

$$f/kT \approx (1 - q\xi_c^2/\sigma)^{1/2}/\xi_c \quad H_c + \delta H_m < H < H_m \quad \text{(III.20)}$$

Matching $f$ in regions (i) and (ii) determines $\delta H_m \approx \xi_c(1 - q\xi_c^2/\sigma)^{-1/2}$. The second boundary of the coexistence region, $H_m$, corresponds to a fully stretched chain of $\xi_s$ blobs; i.e., $H_m \approx (N/g_s)\xi_s \approx N(a/\xi_c)(1 - q\xi_c^2/\sigma)^{1/2}a$. The osmotic interactions reinforce the restoring force. As a result the Pincus blobs are slightly larger than $\xi_c$ while the tension in the chains is somewhat lower than $kT/\xi_c$, the tension in the absence of chain–chain interactions. The main feature is the $f \sim H^0$ dependence in this regime. (iii) A third, final, regime occurs when the bridging chains are fully stretched. The chains are pictured as stretched strings of Gaussian Pincus blobs. However, as opposed to the good solvent case the blob–blob interactions in a poor solvent are attractive. The tension is the chain is due, primarily, to the Gaussian elasticity, with a small correction accounting for the contribution of blob–blob interactions. Altogether we have

$$f/kT \approx H/R_0^2 + (qR_0^2/\sigma)H^{-1} \approx H/R_0^2 \quad \text{(III.21)}$$

In marked distinction to the good solvent behavior, the scaling approach provides a simple description for collapsed brushes with $0 < q < 1$. This description is a slight generalization of the treatment presented in ref 13. As noted above, chain–chain interactions are expected to play a role for $\sigma < \sigma^* \approx Na^2$, when the lateral fluctuations exceed $\sigma^{1/2}$. Chain–chain interactions vanish for $\sigma > \sigma^*$. In this regime the stretching behavior is expected to follow the scheme outlined above with the caveat that osmotic corrections are no longer necessary. In other words, the regime is described by (III.16)–(III.21) with $q = 0$ while the stress is given by $G_N = qf/\sigma$ with $0 < q < 1$. The applicability of this model to the $\sigma < \sigma^*$ regime is less certain since it does not allow for in-plane density modulation due to lateral aggregation of the stretched chains. This type of behavior was first considered by Raphael and de Gennes in a different context: the analysis of rubber–rubber adhesion.[31] A lateral instability was also

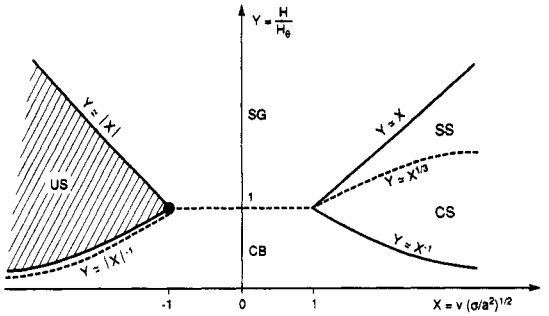


**Figure 2.** State diagram of a lamellar gel.

**Table I**
**Regimes of a Compressed/Stretched Brush**

| | CB | SG | SS | CS |
|---|---|---|---|---|
| $\xi\sigma^{-1/2}$ | $Y$ | $Y^{-1}$ | $X^{1/2}Y^{-3/2}$ | $X^{-1/4}Y^{-3/4}$ |
| $G_N\sigma^{3/2}$ | $Y^{-3}$ | $Y$ | $X^{-1/2}Y^{3/2}$ | $X^{3/4}Y^{9/4}$ |

found by Ross and Pincus,[32] who analyzed a stretched brush immersed in poor solvent using the random-phase approximation. The instability, with regard to lateral aggregation, was found for $\sigma < \sigma^*$. However, the relative importance of the two stretching modes, allowing for the full range of parameters, such as surface interactions, solvent quality, and stress values, is not yet fully established. Finally, it should be emphasized that lamellar mesogels afford unique opportunities for the study of the deformation behavior of polymers immersed in poor solvents. The study of this regime using free chains is hampered by precipitation. The use of a force measurement apparatus capable of lateral motion is complicated by the dynamical nature of the coupling which induces the deformation.

The scaling picture discussed above is presented graphically in Figure 2. The behavior of the brush is characterized in terms of the reduced variables $X = v(\sigma/a^2)^{1/2}$ and $Y = H/H_\Theta \approx H\sigma^{1/2}/Na^2$ for the case $q = 1$. The equilibrium state of the free brush is specified by the dashed line. The regions below the equilibrium line, CS and CB, correspond to a compressed brush. In this regime the free energy of the system is dominated by the interaction term. Blobs exhibiting self-avoidance statistics are expected in the CS region where binary interactions are dominant. Ternary interactions become important in the CB region where the blobs are Gaussian. The boundary between CS and CB is $v \approx Na^3/\sigma H$, as in a semidilute solution of free chains.[8] The regions above the dashed line correspond to a stretched brush. The shaded area, US, denotes the biphasic region with a critical point given by (III.14). The free energy of the stretched brush in the single-phase regions, SG and SS, is dominated by the elastic term. Pincus blobs exhibiting self-avoidance are found in the scaling regime, SS, while Gaussian Pincus blobs occur in SG. A brush stretched in an athermal solvent, $v = 1$, remains within the SS region for all extensions. The crossover between SS and SG for $v < 1$ is specified by $\xi \approx a/v$. The scaling behavior of $\xi$ and $G_N$ in the various regimes is summarized in Table I.

The scaling approach provides a convenient description of lamellar gels swollen by good or Θ solvents in two cases: (i) $q = 1$, (ii) $q < 1$, in the limit of strong deformations. The approach appears to be too rough to account for the weak deformation behavior for $q < 1$. On the other hand, it does provide, with certain limitations noted above, a description of the poor solvent case for all $q$ values. The SCF treatment complements the scaling approach. As we shall see, it enables the analysis of the weak deformation behavior for $q < 1$ in good and Θ solvents. It also confirms the scaling conjectures regarding the strong deformation behavior. However, the two approaches yield slightly different exponents for the good solvent case since the SCF theory theory does not allow for self-avoidance.

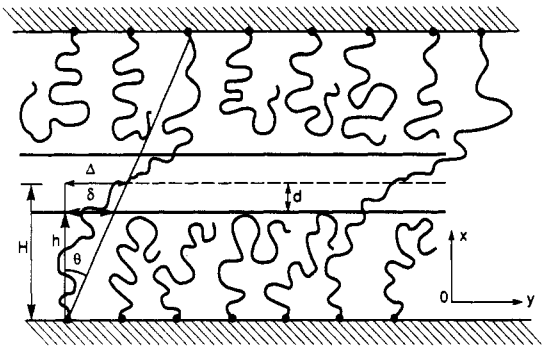


**Figure 3.** Schematic cross section of a lamellar mesogel subject to shear depicting the central region and the two boundary layers. Entangles loops are replaced by two bridging chains. A free loop, comprised of $2N$ monomers, is replaced by two free grafted chains consisting of $N$ monomers per chain.

## IV. Swollen Lamellar Mesogels: SCF Theory

The scaling approach provides partial information on the $q$ dependence of the various characteristics of the gel. A clearer picture may be obtained by implementing an SCF theory along the lines described in section II. However, the theory must be modified to account for the particular features of the problem considered. In this section we focus on the behavior of a lamellar mesogel swollen by a good solvent for the B blocks. Thus, the B layer is no longer in a melt state, and it is necessary to allow for the presence of the solvent. It is assumed that the swelling does not affect the structure of the A domains. In particular, $\sigma$ and $q$ retain their initial values as determined during the preparation of the sample. However, in this case $q$ is treated as a parameter and it is not assumed to reach its equilibrium value. Finally, the treatment must allow for possible deformation of the sample. To account for shear, the free energy is augmented by an extra elastic term due to the in-plane deformation of the coils.

As before it is sufficient to consider half a layer comprised of a boundary layer and a central region. The free energy per chain, $F$, is due to contributions associated with the two regions (Figure 3). The two terms are denoted by $F_b$ and $F_c$, respectively, and $F$ is

$$F = F_b + F_c \tag{IV.1}$$

As before, the bridging chains in the central region are uniformly stretched. The monomer volume fraction within the region $\Phi_c$, is thus constant

$$\Phi_c = q(N - N')a^3/\sigma(H - h) \tag{IV.2}$$

and $F_c$ is

$$F_c/kT = 3q(h - h)^2/2(N - N')a^2 + 3q(\Delta - \delta)^2/2(N - N')a^2 + qv(N - N')^2a^3/\sigma(H - h) \tag{IV.3}$$

The first term accounts for the deformation of the Gaussian chains along the lamellar normal. The possibility of an in-plane, tangential deformation gives rise to the second Gaussian penalty term. This lateral deformation is due to a displacement of the upper A domain by $2\Delta$ with respect to the lower domain. $\delta$ is the lateral displacement of a bridging chain at $x = h$, i.e., at the border between the boundary layer and the central region. The final term, $v(N - N')\Phi$ allows for binary, monomer–monomer inter-

actions in a good solvent. The normal and tangential components of the chain tension $f_{cN}$ and $f_{cT}$ are

$$f_{cN}/kT = 3(H-h)/(N-N')a^2$$

$$f_{cT}/kT = 3(\Delta-\delta)/(N-N')a^2 \qquad \text{(IV.4)}$$

Similar modifications are required for the description of the boundary layer. $F_b/kT$ as given by (II.7) is supplemented by two terms allowing for the in-plane deformation of the bridging chains and for binary monomer–monomer interaction. Altogether $F_b$ is

$$F_b/kT = (1-q)(3/2a^2)\int_0^h d\eta\, g(\eta)\int_0^\eta E_n(x,\eta)\,dx + q(3/2a^2)\int_0^h E_b(x,h)\,dx + q(3/2a^2)\int_0^\delta E_{bT}(y)\,dy + (v\sigma/a^3)\int_0^h \Phi^2(x)\,dx \qquad \text{(IV.5)}$$

where $E_{bT}(y) = dn/dy$ is related to $f_{bT}(y)/kT = (3/a^2)E_{bT}(y)$, the local traverse tension in bridging chains in the boundary layer. Since the chains are assumed to be Gaussian, the normal and traverse deformations, in (IV.5) and (IV.3), are independent. Also, while the interaction free energy is approximated, in both cases, by the binary term, the incorporation of higher order terms is straightforward.[33] $F_b$ is subject to the following constraints:

$$\int_0^\eta E_n^{-1}(x,\eta)\,dx = N \qquad \text{(IV.6)}$$

$$\int_0^h E_b^{-1}(x)\,dx = N' \qquad \text{(IV.7)}$$

$$\int_0^\delta E_{bT}^{-1}(y)\,dy = N' \qquad \text{(IV.8)}$$

and

$$(\sigma/a^3)\int_0^h \Phi(x)\,dx = (1-q)N + qN' \qquad \text{(IV.9)}$$

where $\Phi(x) < 1$ is given by

$$\Phi(x) = (1-q)(a^3/\sigma)\int_x^h g(x,\eta)\,d\eta + qa^3/\sigma E_b(x) \qquad \text{(IV.10)}$$

Constraints (IV.6) and (IV.7) are identical to (II.8) and (II.9). Constraint (IV.8) supplements (IV.7) to assure conservation of monomers in each of the sheared bridging chains. The conservation of monomers within the boundary layer is ensured by constraint (IV.9). This differs from (II.10) which requires a constant melt density. However, the expression for $\Phi(x)$, (IV.10), allowing for the contributions of bridging and nonbridging chains, is identical in the two cases. Matching conditions at the border between the boundary layer and the central region give rise to the following requirements:

$$E_b(h) = (H-h)/(N-N') \qquad \text{(IV.11)}$$

$$E_{bT}(\delta) = (\Delta-\delta)/(N-N') \qquad \text{(IV.12)}$$

$$\Phi(h) = \Phi_c = q(N-N')a^3/\sigma(H-h) \qquad \text{(IV.13)}$$

The equality of tensions on the two sides of the border between the regions is imposed by (IV.11) and (IV.12). Condition (IV.13) assures the continuity of the concentration profile at $x = h$.

The equilibrium state of the B layer, for a given set of $\sigma$, $N'$, $q$, and $\Delta$ corresponds to a minimum of $F$ subject to the listed constraints. The formal details of the calculation are described in Appendix II. The equilibrium state of the boundary layer is specified by

$$E_n(x,\eta) = (\pi/2N)(\eta^2-x^2)^{1/2} \qquad \text{(IV.14)}$$

$$E_b(x) = (\pi/2N)(\Lambda^2-x^2)^{1/2} \qquad \text{(IV.15)}$$

$$E_{bT}(y) = \Delta/N \qquad \text{(IV.16)}$$

$$g(\eta) = \frac{\eta(h^2-\eta^2)^{1/2}}{(1-q)H_0^3}\left[3 + \frac{2qH_0^3}{\pi h \tan(\pi\tau/2)}\frac{1}{\Lambda^2-\eta^2}\right] \qquad \text{(IV.17)}$$

and

$$\Phi(x) = \Phi_0[(1-q\tau)/z + z^2/2 - (3/2)(x/H_0)^2] \qquad \text{(IV.18)}$$

where $\Lambda = h/\cos(\pi\tau/2)$, $\tau = (N-N')/N$, $H_0$ is the thickness of an unperturbed swollen brush of $q = 0$

$$H_0 = (8/\pi^2)^{1/3}v^{1/3}N(a^2/\sigma)^{1/3}a \qquad \text{(IV.19)}$$

$\Phi_0 = Na^3/\sigma H_0$ and $z = h/H_0$. The trajectory of the bridging chains in the boundary layer is obtained from $dx/dy = E_b(x)/E_{bT}(y)$ using (IV.15) and (IV.16)

$$x = [h/\cos(\pi\tau/2)]\sin(\pi y/2\Delta) \qquad \text{(IV.20)}$$

Finally the interdependence of $q\tau$ and $z = h/H_0$ is obtained by combining (IV.11), (IV.14), and (IV.18) keeping in mind that $E_b(h) = qa^3/\sigma\Phi(h)$.

$$2q/\pi \tan(\pi\tau/2) = 1 - q\tau - z^3 \qquad \text{(IV.21)}$$

This is the counterpart of (II.15). However, the state of a swollen gel is specified by three parameters, $q$, $\tau$, and $z$, and it is thus necessary to supplement (IV.21) by another equation.

## V. Force Balance

The primary target of this paper is the $q$ dependence of the swelling equilibrium and the deformation behavior. Force balance considerations enable us to extract the relationships of interest. Mechanical equilibrium requires a balance of the normal and tangential pressures at $x = 0$, the grafting surface at the boundary of the insoluble A domains. The normal component of the stress, $P_N$, is balanced by the normal elastic pressure, $G_N$, and the osmotic pressure, $\Pi$.

$$G_N(x=0) + P_N = \Pi(x=0) \qquad \text{(V.1)}$$

where a positive $P_N$ gives rise to compression of the gel. Since the osmotic pressure has no tangential component, the tangential pressure balance at $x = 0$ is

$$G_T(x=0) = P_T \qquad \text{(V.2)}$$

where $P_T$ is the tangential component of the applied stress and $G_T$ is the tangential component of the elastic pressure in the brush. To proceed, it is necessary to obtain explicit expressions for $G_N$, $G_T$, and $\Pi$ at $x = 0$. The average normal elastic pressure at distance $x < h$ from the grafting surface is

$$G_N(x)/kT = (3/\sigma a^2)(1-q)\int_x^h g(\eta)\,E_n(x,\eta)\,d\eta + (3/\sigma a^2)qE_b(x) \qquad \text{(V.3)}$$

The evaluation of (V.3) is simplified by noting that

$$dG_N(x)/dx = -kT(3\pi^2/4a^5N^2)x\Phi(x) \qquad \text{(V.4)}$$

Consequently

$$G_N(0) - G_N(h) = -\int_0^h (dG_n/dx)\,dx = 3(kT/a^3)v\Phi_0^2\,[(1 - q\tau)/z - z^2/4]z^2 \quad (V.5)$$

where $\Phi_0 = Na^3/\sigma H_0$. Comparison of (IV.11) and (IV.13) yields $G_N(h)a^3/kT = 3q^2(a^2/\sigma)^2\Phi^{-1}(h)$. The osmotic pressure at $x = 0$ is $\Pi a^2/kT = v\Phi^2(0)$, and (V.1) may be rewritten as

$$\frac{3q^2}{(1 - q\tau)/z - z^2} + U_N = \frac{\pi^2}{8}[(1 - q\tau)/z - z^2]^2 \quad (V.6)$$

where $U_N = (P_N a^3/kT)(\sigma/a^2)(Na/H_0)$ is the reduced normal component of the stress. For the tangential component of the elastic pressure, $G_T$, we have $G_T a^3/kT = (q/\sigma)(f_{bT}/kT)$ and, in view of (IV.16), $G_T a^3/kT = 3q(a^2/\sigma)(\Delta/Na)$. It is thus possible to express (V.2) as

$$3qt = U_T \quad (V.7)$$

where $U_T = (P_T a^3/kT)(\sigma/a^2)(Na/H_0)$ and $t = \Delta/H_0$. Since the state of the gel is specified by three dimensionless variables, $z$, $\tau$, and $t$, it is necessary to solve a simultaneous system of three equations: (IV.6), (IV.7), and (IV.21). An expression for $H$ in terms of these variables is needed for the description of the swelling equilibrium. As $H/H_0 = \Phi_0/\Phi$ and $(H - h)/(N - N') = qa^3/\sigma\Phi(h)$, we obtain

$$\frac{H}{H_0} = \frac{1 - z^3}{(1 - q\tau)/z - z^2} \quad (V.8)$$

For comparison purposes it is helpful to consider the dry gel where the layer is in a melt state and $H_0 = Na^3/\sigma$. In this case, the state of the system is determined by (II.15) and (V.7) with an appropriately redefined $t$ and $U_T = (P_T a^3/kT)(\sigma/a^2)^2$.

In the absence of external forces (V.6) is reduced to

$$(1 - q\tau_*)/z_* - z_*^2 = (24/\pi^2)^{1/3}q^{2/3} \quad (V.9)$$

where the subscript asterisk denotes the variables describing the unperturbed system. This, together with (IV.21), specifies the swelling equilibrium of the unperturbed lamellar mesogel. For $q \approx 1$ the system approaches the conditions of the Alexander model. In this limit $\tau_* \approx 1$, $z_* \ll 1$, and (V.9) yields

$$z_* \approx (\pi^2/24)^{1/3}q^{-1}(1 - q^{4/3}) \quad (V.10)$$

In the opposite limit of $q \ll 1$, the B layer is similar to a free brush. The central region is small, $\tau_* \approx 1$ and $H/H_0 \approx 1$. In this case (V.8) leads to

$$z_* \approx 1 - (24/3^3\pi^2)^{1/3}q^{2/3} \quad (V.11)$$

and the combination of (V.8) and (V.9) leads to

$$\tau_* \approx (8/3\pi^4)^{1/3}q^{1/3} \quad (V.12)$$

A somewhat different $q$ dependence is found in dry gels. In the $q \approx 1$ limit (II.4) leads to

$$z_* \approx 1 - q \quad (V.13)$$

In the $q \ll 1$ limit we obtain

$$\tau_* \approx (2/\pi)^2 q \quad (V.14)$$

by expanding $(1 - q\tau)\tan(\pi\tau/2)$, matching the resulting expression with a polynominal in $q$ and substituting the result in (II.15). The combination of (V.14) and (II.4) leads to

$$z_* \approx 1 - (2/\pi)^2 q^2 \quad (V.15)$$

The numerical solutions for $z_*(q)$ and $\tau_*(q)$ for dry and swollen gels are depicted in Figure 4. A similar smooth crossover between the free brush limit and the Alexander model behavior is exhibited in the plots of $H_*/H_0$ and $\Phi_*/\Phi_0$ shown in Figure 5. The concentration profile and the free ends distribution function, as obtained from (IV.17) and (IV.18), are depicted in Figures 6 and 7.

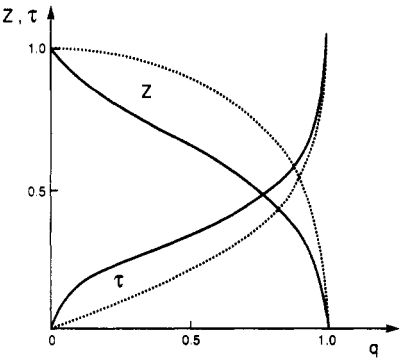


**Figure 4.** Plot of $z$ and $\tau$ vs $q$ for "dry" (dotted line) and swollen (solid line) B layers.

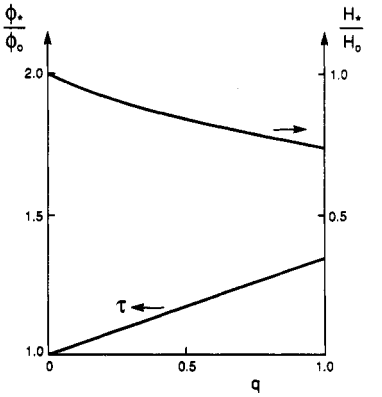


**Figure 5.** Plot of $\Phi_*/\Phi_0$ and $H_*/H_0$ vs $q$.

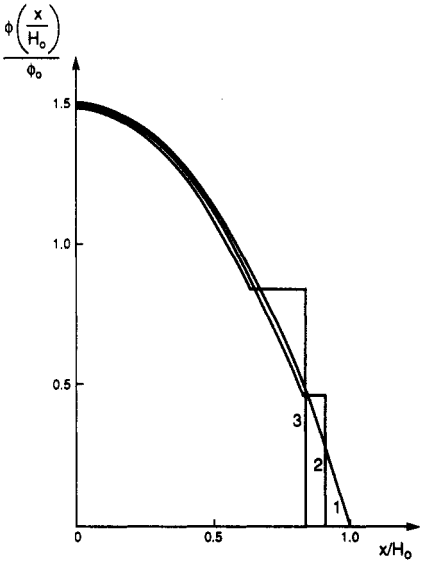


**Figure 6.** Profiles of the monomer volume fraction, $\Phi(x)$, in swollen B layers for (1) $q = 0.0$, (2) $q = 0.2$, and (3) $q = 0.5$.

The Hookean behavior of a lamellar gel subject to weak external forces is characterized by Young's and shear moduli. Young's modulus, $E$, specifies the linear extension of a gel stretched by a force acting along the lamellar normal. For a normal stress $P_N$ and a normal stress of $\epsilon = (H - H_*)/H_* \ll 1$ Young's modulus is given by

$$E = dP_N/d\epsilon \quad (V.16)$$

This leads to $Ea^3/kT = (8/\pi^2)v\Phi_0^2(dU_N/dz)_*/(d\epsilon/dz)_*$ and, using (V.6) and (V.8), to

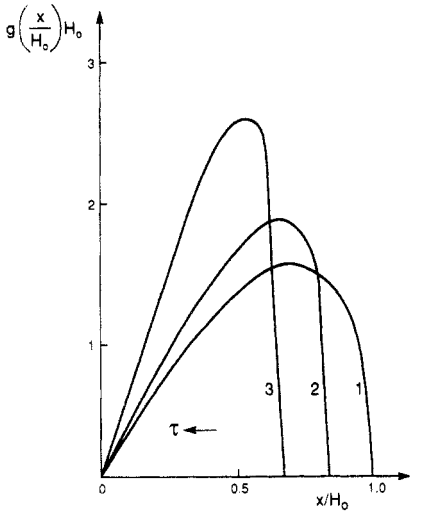


**Figure 7.** Free ends distribution function, $g(\eta/H_0)$ for (1) $q$ = 0.0, (2) $q$ = 0.2, and (3) $q$ = 0.5.

$$Ea^3/kT = 12v\Phi_0^2(3q^2/\pi^2)^{1/3}[z_*^2 + (3q^2/\pi^2)^{1/3}]/[3 - 2/(1 - z_*^3) + z_*^2(\pi^2/3q^2)^{1/3}] \quad \text{(V.17)}$$

In the limit of $q \ll 1$ (V.18) and (V.11) lead to

$$Ea^3/kT \approx v\Phi_0^2 q^{2/3} \quad \text{(V.18)}$$

This result can be easily derived by balancing the increment of the normal stress per chain, $dP_N\sigma/q$, with the increment of the elastic restoring force per chain. For $q \ll 1$ the boundary layer is hardly affected and the Gaussian restoring force is dominated by the chain segment in the central region, $kTdH/\tau Na^2$. Since in this limit $E = dP_N H_0/dH$, we obtain $Ea^3/kT \approx (H_0/a\sigma)(q/\tau N) \approx \Phi_0^2 q^{2/3}$.

The shear modulus, $n$, characterizes the relative displacement of the lamellae due to a force acting along the lamellar plane. For a shear stress $P_T$ and shear strain $\Theta = \Delta/H_* \approx \Delta/H_0 \equiv t$ we have

$$n = dP_T/dt \quad \text{(V.19)}$$

Since $P_T a^3/kT = (8/\pi^2)^{1/3}(a^2/\sigma)^{4/3}v^{1/3}U_T$, (V.7) leads to

$$na^3/kT = (24/\pi^2)v\Phi_0^2 q \quad \text{(V.20)}$$

As before, (V.20) may be derived by equating the incremental restoring force per chain, $kTd\Delta/Na^2$, to the shear stress per chain, $dP_T/\sigma q$. This leads to $n = dP_T H_*/D\Delta \approx \Phi_0^2 q$.

In the dry gel, where $\Theta = t = \Delta/H_0$, $H_0 = Na^3/\sigma$, and $P_T a^3/kT = (a^2/\sigma)^2 U_T$, $n$ is

$$na^3/kT = 3(a^2/\sigma)^2 q \quad \text{(V.21)}$$

Since the chains are considered to be Gaussian within the SCF approach, pure shear does not affect the structure of the layer along the lamellar normal; i.e., there is no effect on $z$ and $\tau$ even for strong deformations. Note that $n$ and $E$ are not simply proportional since the lamellar gel is not isotropic.

The SCF results concerning $H/H_*$, $\tau$, and $z$ (Figures 7–11) confirm our expectations[3] concerning the strong deformation behavior of lamellar mesogels. The relevant features are as follows: (i) The effect of compression on $\tau$ and $z$ is weakly dependent on $q$. The behavior of the B layer for $q < 0.1$ is barely distinguishable from that of a free brush subject to compression. (ii) Stretching has a weak effect on the boundary layer. However, the central region dominates the structure of the B layer even for weak stretching. Thus, the stretched gel is well described by the Alexander model for stretched brushes (section III) if the area per chain is taken to be $\sigma/q$ rather than $\sigma$. Altogether, $E$ is expected to scale as $q^{2/3}$ for weak deformations, as $q$ for strong stretching, and as $q^0$ for strong compression.

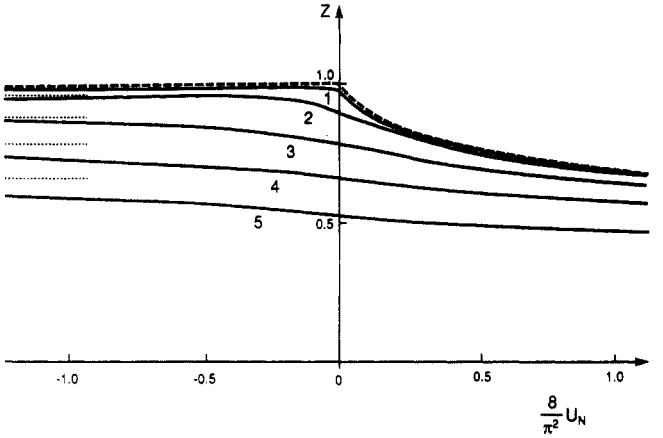


**Figure 8.** Plots of $z$ vs $U_N$ for (1) $q$ = 0.01, (2) $q$ = 0.1, (3) $q$ = 0.3, (4) $q$ = 0.5, and (5) $q$ = 0.7. The dashed line corresponds to a free brush ($q$ = 0) and the dotted line to the asymptotic value of $z$ at $U_N = \infty$.

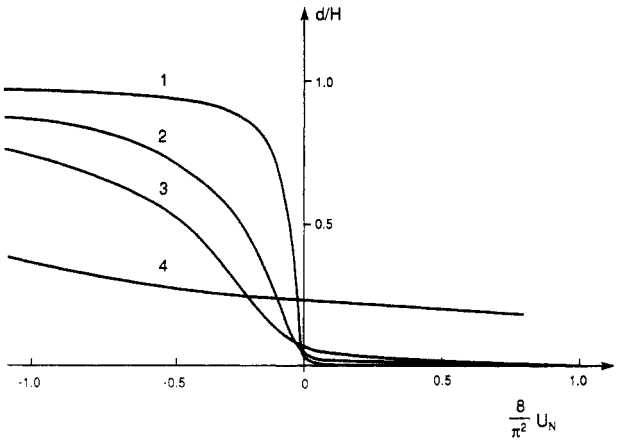


**Figure 9.** Relative thickness of the central zone, $d/H_0$, vs $U_N$ for (1) $q$ = 0.01, (2) $q$ = 0.05, (3) $q$ = 0.1, and (4) $q$ = 0.5.

## VI. Discussion

The SCF theory of lamellar mesogels enables the analysis of problems which are difficult to treat via the Alexander approach. The scaling behavior of the equilibrium bridging fraction, (II.19), may be difficult to observe since the systems may fail to attain complete thermodynamical equilibrium. On the other hand, the $q$ dependence of the elastic moduli may provide a useful probe of the actual bridging fraction. For weak deformations, we expect Young's modulus to scale as $E \sim q^{2/3}$, (V.18), and the shear modulus to scale as $n \sim q$ (V.20).

Fluctuations may affect some of our conclusions. In particular, the central region may be smeared out in the melt case. It is however expected to survive, as a well-defined zone, in the swollen mesogel. The smearing results from the penetration of free ends into the central region. The penetration length, $\xi$, may be identified with the thickness of the weakly stretched region of the parabolic profile of the boundary layer. The number of monomers deposited by a chain in this region, $n$, is $n/N = \int_{h-\xi}^{h} E_b^{-1}(x) = 1 - (2/\pi)\arcsin(1 - \xi/h) \approx (2/\pi)(2\xi/h)^{1/2}$. Since this segment is only weakly deformed, $\xi$ is given by $\xi = na^2$. By comparing the two expressions, we find $\xi/H \approx (aN^{1/2}/h)^{4/3}$. The importance of the fluctuations can be

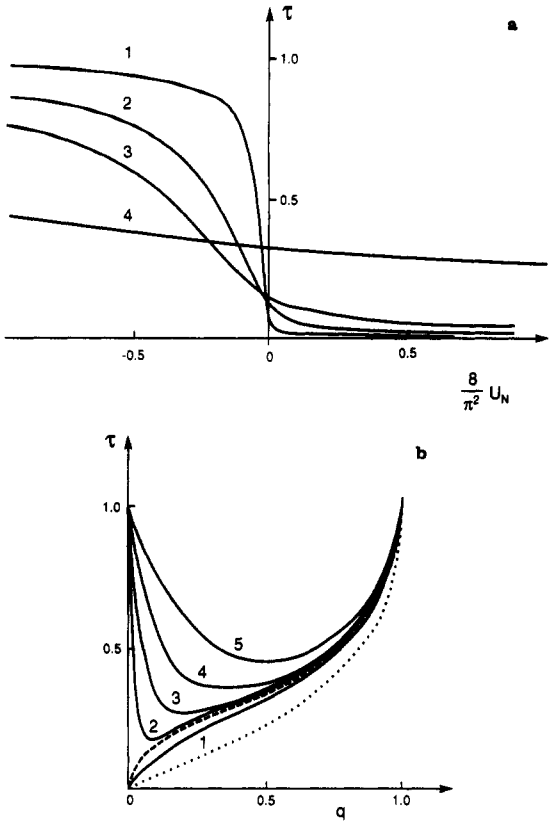


**Figure 10.** Plots of (a) $\tau$ vs $(\pi^2/8)U_N$ for $q$ values of (1) 0.01, (2) 0.05, (3), 0.10, and (4) 0.50 and of (b) $\tau$ vs $q$ for $(\pi^2/8)U_N$ values of (1) 0.20, (2) −0.05, (3) −0.20, (4) −0.50, and (5) −1.00. The dotted and dashed lines corresponded respectively to $U_N = \infty$ and $U_N = 0$.

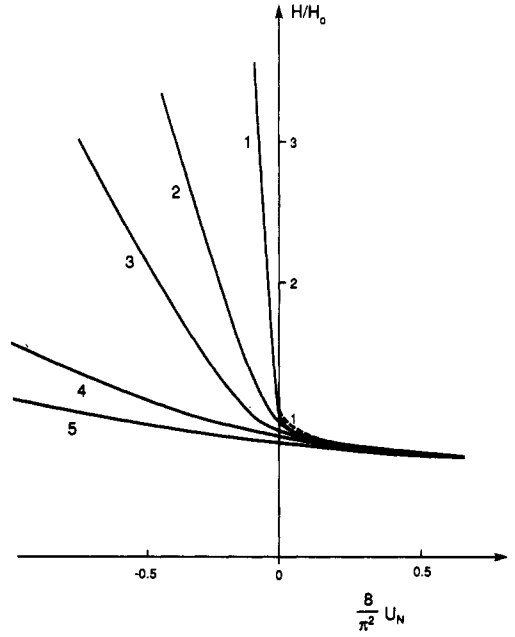


**Figure 11.** Plots of $H/H_0$ vs $U_N$ for (1) $q = 0.01$, (2) $q = 0.05$, (3) $q = 0.1$, and (4) $q = 0.5$. The dashed line corresponds to a free brush ($q = 0$).

estimated by comparing $\xi$ to the thickness of the central region $d = H - h$. Focusing on the case of $q \ll 1$ such that $h \approx H_0$, we have, in view of (II.4) and (V.14), $d/h = q\tau \approx q^2$. For $q = q_{eq}$ we thus have $d \approx N^{1/3}(\sigma/a^2)^{1/3}$ and $\xi \approx d$; i.e., fluctuations are important, and the central region may be smeared out. A distinct central region may occur providing $q \ll q_{eq}$. For a swollen gel $\xi/H \approx \sigma^{4/9}/N^{2/3}a^2$ while $d/H \approx q^{2/3}$ (from (V.9) in the limit of $q \ll 1$). For $q = q_{eq}$ we thus have $d/\xi \approx N^{2/3}/N^{2/9} \gg 1$ suggesting that fluctuations do not play an important role in this case.

The formation of birefringent, multicrystalline mesogels was observed by Skoulios et al.[35] and by Franta et al.[36] upon mixing ABA triblock copolymers in a selective solvent. In their case the A domains were crystalline. It was possible to obtain lamellar, cylindrical, and micellar mesogels by changing the polymer concentration. Single-crystal samples of lamellar and cylindrical mesogels were reported by Folkes et al.[5,37,38] In these experiments an ABA melt mesophase was aligned by a shear field. The swelling behavior was studied after the sample was cooled below the $T_g$ of the A domains. Anisotropic swelling was indeed observed for lamellar[37] and cylindrical mesogels.[5,38] However, extensive swelling caused breakup of the A domains. This was associated with the onset of isotropic swelling and by loss of reversibility; i.e., upon deswelling the gel did not recover the initial state. The experiments of Folkes et al. provide a starting point for a systematic study of mesogels. However, it is necessary to use robust samples, capable of reaching equilibrium swelling and withstanding deformation with no disruption of the A domains. It is possible to enhance the robustness of the samples by increasing the size of the A domains by using copolymers with longer A blocks, choosing A blocks with higher $T_g$, optimizing the choice of the selective solvent, and inducing selective cross-linking in the A domains. It is also possible to improve the alignment of the sample by using oscillatory rather than simple shear fields.[39] It is, of course, important to prepare a series of samples, with blocks of different size, to enable to study of the $N$ and $\sigma$ dependence.

Swelling experiments, designed to test the $c^*$ theorems characterizing the swelling equilibria of the various mesogels,[3,4] are the simplest to perform. In these experiments one benefits from the weak $q$ dependence of the phenomenon. The study of the force law characterizing the compression behavior affords the same advantage. However, the compression of lamellar and cylindrical mesogels, with no disruption of the A domains, is accompanied by a change of volume. In turn, the associated hydrodynamical equilibration makes for time-consuming experiments. Since the stretching behavior is very sensitive to $q$, one may combine compression and stretching experiments to probe the fraction of bridging chains. The difficulties due to hydrodynamical equilibration of gels subject to deformation may be circumvented by studying shear-induced deformation, where the volume of the sample is constant. However, in this case it is necessary to determine $q$ by using a different method. Dielectric relaxation may be used, in certain cases, to this end. In particular, the B monomers should have an electric dipole aligned along the chain contour.[40,41] For such systems one may obtain a measure of $q$ by comparing the behavior of a sample of $A_MB_{2N}A_M$ triblock copolymers and a sample of $A_MB_N$ diblock copolymers. This type of experiment is of interest in its own right as a "low tech" probe of $q$.

Finally, lamellar mesogels afford unique opportunities for the study of deformed polymer chains under static conditions. In particular, it should be possible to study the nonlinear Pincus regime of strongly deformed chains in a good solvent. Lamellar gels also enable the study of the deformation behavior of brushes in poor solvents. In both cases the simplest experiments concern mechanical measurement designed to probe the stress–strain diagram. However, it is also possible to study the deformed chains by means of small-angle neutron scattering. Such experiments face serious difficulties because of the strong

background due to the periodic structure. However, they offer a unique opportunity to study the strong deformation regime where the correlation length, in a good solvent, is determined by the applied force rather than the concentration.

**Acknowledgment.** We acknowledge, with thanks, support and assistance from several sources during the preparation of this article. E.B.Z. and A.H. acknowledge the hospitality of Professors E. W. Fischer and G. Wegner of the Max-Planck-Institut für Polymerforschung. E.B.Z. acknowledges the hospitality of Professor K. Binder of the Johannes Gutenberg University, Mainz, Germany, and financial support provided by the Alexander von Humboldt Foundation. A.H. acknowledges the hospitality of Professor Pincus of UCSB and financial support provided by Ford Motor Co. and by DOE Grant No. DE-FG03-87ER45288. We also acknowledge with gratitude helpful discussions with H. Benoit, R. Ball, P.-G de Gennes, A. Keller, P. Pincus, E. Raphael, and R. Ross. T. M. Birshstein and O. Borisov pointed out the independence of the normal and tangential deformations of the bridging chains.

## Appendix I

The equilibrium state of the layer minimizes $F$, (II.7), subject to the constraints (II.8), (II.9), and (II.10). The constraints may be treated by means of the Lagrange method of undetermined multipliers. The equilibrium state corresponds thus to the stationary value of

$$\Omega = F/kT + \int_0^h d\eta\, \tilde{\lambda}(\eta) \int_0^\eta \frac{dx}{E_n(x,\eta)} + \tilde{\omega} \int_0^h \frac{dx}{E_b(x)} + \int_0^h dx\, \tilde{\psi}(x) \left[ (1-q)\frac{a^3}{\sigma} \int_x^h \frac{g(\eta)\, d\eta}{E(x,\eta)} + q\frac{a^3}{\sigma}\frac{1}{E_b(x)} \right] \quad (A.1)$$

where $\tilde{\lambda}$, $\tilde{\omega}$, and $\tilde{\psi}$ are the Lagrange multipliers associated with constraints (II.8), (II.9), and (II.10), respectively. The fourth term is rearranged by changing the order of integration and, accordingly, the domains of integration. This and the incorporation of numerical factors into the Lagrange multipliers yields

$$\Omega = (1-q)(3/2a^2) \int_0^h d\eta \int_0^\eta dx\, I(x,\eta) + q(3/2a^2) \int_0^h dx\, J(x) \quad (A.2)$$

where

$$I = g(\eta)\, E_n(x,\eta) + \lambda(\eta) E_n^{-1}(x,\eta) + \psi(x)\, g(\eta)\, E_n^{-1}(x,\eta) \quad (A.3)$$

and

$$J = E_b(x) + \omega E_n^{-1}(x) + \psi(x)\, E_n^{-1}(x) \quad (A.4)$$

The first order variation with respect to $E_n$ and $E_b$ yields

$$g(\eta) - \lambda(\eta)\, E_n^{-2}(x,\eta) - \psi(x)\, g(\eta)\, E_n^{-2}(x,\eta) = 0 \quad (A.5)$$

$$1 - \omega E_b^{-2}(x) - \psi(x)\, E_b^{-2}(x) = 0 \quad (A.6)$$

Upon rewriting (A.5) as

$$E_n^2(x,\eta) = \lambda(\eta)/g(\eta) + \psi(x) \quad (A.7)$$

and using the condition $E_n(\eta,\eta) = 0$, we find that $\lambda(\eta)/g(\eta) = \psi(\eta)$ and accordingly

$$E_n(x,\eta) = [\psi(\eta) - \psi(x)]^{1/2} \quad (A.8)$$

Substitution of (A.8) into (II.8), followed by a change of variables $\psi(x) = t$, $\psi(\eta) = \rho$, and $dx = f(t)\, dt$ yields an Abel type integral equation.[42,43] The solution $f(t) = \pi/Nt^{1/2}$ or equivalently

$$\psi(x) = (\pi/2N)^2 x^2 \quad (A.9)$$

leads to (II.12). Substitution of $\psi(x)$ into (A.6) yields

$$E_b(x) = (\pi/2N)(\Lambda^2 - x^2)^{1/2} \quad (A.10)$$

which $\Lambda$, as determined by the constraint (II.9), is

$$\Lambda = h/\sin(\pi N'/2N) \quad (A.11)$$

The matching condition at $h$, $E_b(h) = (L-h)/(N-N')$, together with (II.4) leads to (II.15).

Knowing $E_b(x)$ and $E_n(x,\eta)$, we can determine $g(\eta)$ from constraint (II.10). Following a change in variables, $h^2 - x^2 = \xi$, $h^2 - y^2 = \rho$, and $(1-q)g(\eta)\, d\eta = -p(\rho)\, d\rho$, we may rewrite (II.10) as an Abel integral equation

$$\int_0^\xi p(\rho)\, (\xi - \rho)^{-1/2}\, d\rho = f(\xi) \quad (A.12)$$

where $f(\xi) = \pi\sigma/2Na^3 - q(A^2 + \xi)^{-1/2}$ and $A^2 = \Lambda^2 - h^2$. This is solved by

$$p(\xi) = \frac{1}{\pi}[B\xi^{-1/2} + (q/2) \int_0^\xi (\xi - t)^{-1/2}(A^2 + t)^{-3/2}\, dt] \quad (A.13)$$

where $B = \tau\sigma/2Na^3 - q/A$ vanishes identically because of the matching condition $E_b(h) = (\pi/2N)A = (L-h)/(N-N')$. Integration, following change of variable to $z = (A^2 + t)^{-1}$, yields

$$g(\eta) = \frac{2}{\pi}\frac{q}{1-q}\frac{\eta}{\Lambda^2 - y^2}\left[\frac{h^2 - \eta^2}{\Lambda^2 - h^2}\right] \quad (A.14)$$

This reduces to (II.14) by using (II.4), (II.13), and the matching condition.

To obtain $F_b/kT$, we rewrite it, after changing the order of integration and, consequently, the domains of integration, as

$$F_b/kT = (3/2a^2)(\pi/2N) \int_0^h f(x)\, dx \quad (A.15)$$

where

$$f(x) = (1-q) \int_x^h g(\eta)\, (\eta^2 - x^2)^{1/2}\, d\eta + q(\Lambda^2 + x^2)^{1/2} \quad (A.16)$$

Comparison with (II.10) shows that $f' = df/dx$ is equal to $f'(x) = -x\Phi(x)\, (\pi\sigma/2Na^3)$. However, in our case $\Phi(x) = 1$, and a result

$$f'(x) = -x(\pi\sigma/2Na^3) \quad (A.17)$$

Since $f(x) = -\int_x^h f'(t)\, dt + f(h)$, $F_b$ is

$$F_b/kT = (\pi^2\sigma/8a^5)N^{-2}h^3 + (3\pi/4Na^2)qh(\Lambda^2 - h^2)^{1/2} \quad (A.18)$$

By utilizing the matching condition and (II.4), we get $F_{el} = F_b + F_c$ as expressed in (II.16).

## Appendix II

The equilibrium state of the layer corresponds to a minimum in $F$, (II.5), subject to the constraints (IV.6), (IV.7), and (IV.9) as obtained by means of the Lagrange method of undetermined multipliers. The equilibrium

state corresponds thus to the stationary value of

$$\Omega = F/kT + \int_0^h d\eta\, \tilde{\lambda}(\eta) \int_0^\eta \frac{dx}{E_n(x,\eta)} + \tilde{\omega} \int_0^h \frac{dx}{E_b(x)} + \tilde{\omega}_T \int_0^h \frac{dy}{E_{bT}(y)} + \int_0^h dx\, \tilde{\mu}\left[(1-q)\frac{a^3}{\sigma}\int_x^h \frac{g(\eta)\, d\eta}{E_n(x,\eta)} + q\frac{a^3}{\sigma}\frac{1}{E_b(x)}\right] \quad (B.1)$$

where $\tilde{\lambda}$, $\tilde{\omega}$, $\tilde{\omega}_T$, and $\tilde{\mu}$ are the Lagrange multipliers associated with constraints (IV.6), (IV.7), (IV.8), and (IV.9), respectively. The fourth term is rearranged by changing the order of integration and, accordingly, the domains of integration. This and the incorporation of numerical factors into the Lagrange multipliers yields

$$\Omega = (1-q)(3/2a^2)\int_0^h d\eta \int_0^\eta dx\, I(x,\eta) + q(3/2a^2)\int_0^h dx\, J(x) + (\sigma v/a^3)\int_0^h dx\, \Phi^2(x) + q(3/2a^2)\int_0^\delta M(y)\, dy \quad (B.2)$$

where

$$I = g(\eta)\, E_n(x,\eta) + \lambda(\eta)\, E_n^{-1}(x,\eta) + \mu g(\eta)\, E_n^{-1}(x,\eta) \quad (B.3)$$

and

$$J = E_b(x) + \omega E_b^{-1}(x) + \mu E_b^{-1}(x) \quad (B.4)$$

$$M = E_{bT}(y) + \omega_T E_{bT}^{-1}(y) \quad (B.5)$$

The first order variation with respect to $E_n$ and $E_b$ yields

$$g(\eta) - \lambda(\eta) E_n^{-2}(x,\eta) - \psi(x)\, g(\eta)\, E_n^{-2}(x,\eta) = 0 \quad (B.6)$$

$$1 - \omega E_b^{-2}(x) - \psi(x)\, E_b^{-2}(x) = 0 \quad (B.7)$$

with

$$\psi(x) = \mu + (4va^3/3)\Phi(x) \quad (B.8)$$

and

$$1 - \omega_T E_b^{-2} = 0 \quad (B.9)$$

$E_n(x,\eta)$ and $E_b(x)$ are obtained exactly as in Appendix I. With $\Phi(x)$ given by (A.9) the functional form of $\Phi(x)$ is determined. The value of $\mu$ is set by constraint (IV.9). $g(\eta)$ is obtained as in Appendix I, using $\Phi$ as given by (IV.10) rather than $\Phi = 1$. (B.9) and constraint (IV.8) yield $E_{bT} = \delta/N'$, which reduces to (IV.16) when the matching condition (IV.12) is invoked.

## References and Notes


(1) (a) Benoit, H.; Hadziioannou, G. *Macromolecules* **1988**, *21*, 1449. (b) Hadziioannou, G.; Skoulios, A. *Macromolecules* **1982**, *15*, 258; **1982**, *15*, 263; **1982**, *15*, 267.
(2) Legge, N. R.; Holden, G., Schroeder, H. E. Eds. *Thermoplastic Elastomers*; Hanser Publishers: Munich, 1987.
(3) Halperin, A.; Zhulina, E. B. *Europhys. Lett.* **1991**, *16*, 337.
(4) Halperin, A.; Zhulina, E. B. *Prog. Colloid Polym. Sci.*, in press.
(5) Keller, A.; Odell, J. A. In *Processing, Structure and Properties of Block Copolymers*; Folkes, M. J., Ed.; Elsevier: New York, 1985.
(6) Halperin, A.; Tirrell, M.; Lodge, T. P. *Adv. Polym. Sci.* **1992**, *100*, 31.
(7) Candau, S.; Bastide, J.; Delsanti, M. *Adv. Polym. Sci.* **1982**, *44*, 30.
(8) de Gennes, P.-G. *Scaling Concepts in Polymer Physics*; Cornell University Press: Ithaca, NY, 1979.
(9) Semenov, A. N. *Sov. Phys. JETP* **1985**, *61*, 731.
(10) Ross-Murphy, S. B., Burchard, W., Eds. *Physical Networks—Polymers and Gels*; Elsevier Applied Science: London, 1990.
(11) He, X.; Herz, J.; Guenet, J. M. *Macromolecules* **1987**, *20*, 2003; **1988**, *21*, 1557; **1989**, *22*, 1390.
(12) Halperin, A.; Zhulina, E. B. *Europhys. Lett.* **1991**, *15*, 417.
(13) Halperin, A.; Zhulina, E. B. *Macromolecules* **1991**, *24*, 5393.
(14) Birshtein, T. M.; Zhulina, E. B. *Polym. Sci. (USSR)* **1985**, *27*, 1613.
(15) Alexander, S. *J. Phys. (Fr.)* **1977**, *38*, 977.
(16) Milner, S. T.; Witten, T. A.; Cates, M. E. *Europhys. Lett.* **1988**, *5*, 413; *Macromolecules* **1988**, *21*, 2610.
(17) Johner, A.; Joanny, J. F. *Europhys. Lett.* **1991**, *15*, 265.
(18) Ligoure, C.; Leibler, L.; Rubinstein, M. *Macromolecules*, in press.
(19) Zhulina, E. B.; Pakula, T. *Macromolecules*, in press.
(20) Doi, M.; Edwards, S. F. *The Theory of Polymer Dynamics*; Clarendon Press: Oxford, U.K., 1990.
(21) Witten, T.; Cohen, M. H. *Macromolecules* **1985**, *18*, 1915.
(22) Cates, M. E.; Turner, M. S. *Europhys. Lett.* **1990**, *11*, 681.
(23) Birshtein, T. M.; Zhulina, E. B. *Polymer* **1990**, *31*, 1312.
(24) Rabin, Y.; Alexander, S. *Europhys. Lett.* **1990**, *13*, 49.
(25) Pincus, P. *Macromolecules* **1986**, *9*, 386.
(26) Lifshits, I. M.; Grosberg, A. Y.; Khokhlov, A. R. *Rev. Mod. Phys.* **1978**, *50*, 683.
(27) Williams, C.; Borchard, F.; Frisch, H. L. *Annu. Rev. Phys. Chem.* **1981**, *32*, 433.
(28) Halperin, A. *J. Phys. Fr.* **1988**, *47*, 547.
(29) Shim, D. F. K.; Cates, M. E. *J. Phys. Fr.* **1989**, *50*, 3535.
(30) (a) Birshtein, T. M.; Zhulina, E. B. *Polym. Sci. USSR* **1983**, *25*, 2165. (b) Zhulina, E. B.; Borisov, O. V.; Priamitsin, V. A.; Birshtein, T. M. *Macromolecules* **1991**, *24*, 140. (c) Borisov, O. V.; Birshtein, T. M.; Zhulina, E. B. *Polym. Sci. USSR* **1980**, *30*, 767.
(31) Raphael, E.; de Gennes, P.-G. *Macromolecules*, in press.
(32) Ross, R. S.; Pincus, P. *Europhys. Lett.* **1992**, *19*, 79.
(33) Birshtein, T. M.; Liatskaya, Yu. V.; Zhulina, E. B. *Polymer* **1991**, *31*, 2185.
(34) Zhulina, E. B.; Semenov, A. N. *Vyskomol. Soedin* **1989**, *A31*, 177.
(35) Skoulious, A.; Tsouladze, G.; Franta, E. *J. Polym. Sci.* **1963**, *64*, 507.
(36) Franta, E.; Skoulios, A.; Rempp, P.; Benoit, H. *Makromol. Chem.* **1965**, *87*, 271.
(37) Folkes, M. J.; Keller, A.; Odell, J. A. *J. Polym. Sci., Polym. Phys. Ed.* **1976**, *14*, 833.
(38) Folkes, M. J.; Keller, A.; Odell, J. A. *J. Polym. Sci., Polym. Phys. Ed.* **1976**, *14*, 847.
(39) Hadziioannou, G.; Mathis, A.; Skoulios, A. *Colloid Polym. Sci.* **1979**, *257*, 136.
(40) Stockmayer, W. *Pure Appl. Chem.* **1967**, *15*, 247.
(41) Boese, D.; Kremer, F.; Fetters, L. J. *Macromolecules* **1990**, *23*, 1826.
(42) Bronshtein, I. N.; Semendydyev, K. A. *Handbook of Mathematics*; Van Nostrand Reinhold: New York, 1985.
(43) The Abel integral equation $f(x) = \int_a^x [\Phi(s)\, ds/(x-s)^{1}1/2]$ is solved by

$$\Phi(x) = \frac{1}{\pi}\left[\frac{f(a)}{(x-a)^{1/2}} + \int_a^x \frac{f'(s)\, ds}{(x-s)^{1/2}}\right]$$